Available online at www.sciencedirect.com
ScienceDirect
Trans. Nonferrous Met. Soc. China 27(2017) 829−838
Transactions of Nonferrous Metals Society of China
www.tnmsc.cn

Wear behavior of Ti6Al4V biomedical alloys processed by selective laser melting, hot pressing and conventional casting

F. BARTOLOMEU[1], M. BUCIUMEANU[2], E. PINTO[3], N. ALVES[3], F. S. SILVA[1], O. CARVALHO[1], G. MIRANDA[1]

1. Center for Micro-Electro Mechanical Systems (CMEMS-UMinho), University of Minho, Azurém, 4800-058 Guimarães, Portugal;
2. Cross-Border Faculty of Humanities, Economics and Engineering, "Dunărea de Jos" University of Galaţi, Domnească 47, 800008 Galati, Romania;
3. Centre for Rapid and Sustainable Product Development Polytechnic Institute of Leiria, Rua General Norton de Matos, Apartado 4133, 2411-901 Leiria, Portugal

Received 5 April 2016; accepted 2 June 2016

Abstract: The aim of this work was to study the influence of the processing route on the microstructural constituents, hardness and tribological (wear and friction) behavior of Ti6Al4V biomedical alloy. In this sense, three different processing routes were studied: conventional casting, hot pressing and selective laser melting. A comprehensive metallurgical, mechanical and tribological characterization was performed by X-ray diffraction analysis, Vickers hardness tests and reciprocating ball-on-plate wear tests of Ti6Al4V/Al_2O_3 sliding pairs. The results showed a great influence of the processing route on the microstructural constituents and consequent differences on hardness and wear performance. The highest hardness and wear resistance were obtained for Ti6Al4V alloy produced by selective laser melting, due to a markedly different cooling rate that leads to significantly different microstructure when compared to hot pressing and casting. This study assesses and confirms that selective laser melting is potential to produce customized Ti6Al4V implants with improved wear performance.

Key words: biomedical alloy; Ti6Al4V alloy; wear behavior; microstructure; selective laser melting; hot pressing; casting

1 Introduction

Titanium and its alloys are widely used in orthopaedic and dental implants. These alloys have remarkable properties, suited for biomedical applications like implants, as a high corrosion resistance, high strength and excellently soft and hard tissue biocompatibility [1,2]. On the other hand, it is known that the main disadvantage of titanium alloys is their poor wear resistance [3,4]. Implants failure is mostly attributed to a weak interfacial bond between implant surface and living tissue and to wear-induced osteolysis [5−7]. In the case of total hip replacement, the micro-motions that occur at the contact between bone and implant can lead to wear-induced osteolysis [5,6,8]. In this sense, a high wear resistance is required for orthopedic implants to achieve biocompatibility and acceptability [6]. Consequently, in the last decades, considerable effort has been made to improve the wear resistance of titanium and its alloys by using several surface modification techniques [4,9−12]. Regarding Ti6Al4V alloy, the most commonly used titanium alloy for biomedical applications [10,12], different processing methods have been tested as viable: casting processes, powder metallurgy, thermal spraying, laser sintering and laser melting, among others [13−18].

The low flexibility of casting technology in terms of geometry and materials design, the difficulty to produce parts with local requirements and often the need to perform thermal or mechanical processing after manufacturing [14,19,20] are their main disadvantages. Regarding Ti6Al4V alloy fabricated by casting, other drawbacks arise, like the requirement of suited crucible and mold materials and a high reactivity (e.g., oxidation problem, phase transition, decomposition, grain growth) [21]. Regarding the wear behavior of Ti6Al4V alloy produced by casting [22−25], it has been reported that the wear resistance of this alloy is rapidly decreased due to the presence of loosen oxide layer [26]. It has also

Corresponding author: F. BARTOLOMEU; E-mail: flaviojorgebartolomeu@gmail.com
DOI: 10.1016/S1003-6326(17)60060-8

been stated that deep grooves, gross plastic deformation (even under low loads) [23], severe delamination and severe adhesion are usual on the worn surface of cast Ti6Al4V alloy [26].

Hot pressing (HP) is a powder metallurgy process that combines pressure and temperature simultaneously (HP sintering stage). HP provides a simpler production route with better mechanical and electrochemical properties as compared to the conventional techniques [17,18,26]. The wear behavior of biomaterials in general and Ti6Al4V in particular produced by HP has been reported superior to that produced by casting [17,18].

Selective laser melting (SLM) technology is an additive manufacturing process which allows the production of complex 3D parts directly from CAD data using a laser beam that melts powder beds layer by layer [27−29]. SLM technology allows the production of almost full density parts with good dimensional accuracy and high mechanical properties [30,31]. The majority of Ti6Al4V prostheses are currently obtained by forging or casting [32]; however, there is an opportunity to apply SLM technique to easily and quickly produce customized implants, suited to the patient, not possible by using traditional manufacturing technologies.

Depending on the processing steps during manufacturing, a metallic material microstructure may vary substantially, and consequently display very different mechanical and physical properties and also distinct wear resistance [30]. Ti6Al4V alloy is organized in a β phase above the $\beta_{transus}$ temperature (typically above 950 °C) and in an α+β phase below this temperature [33]. Then, the amount of retained β phase is dictated by the cooling rate experienced by the material. In the case of SLM production of each layer, the cooling rate is very high (10^3−10^8 K/s) [34,35] when compared with casting and HP technologies. In this context, the microstructures of Ti6Al4V parts produced by selective laser melting, are expected to be significantly different to those produced by hot pressing and conventional casting, which can lead to distinct wear behaviours.

This work aims to investigate the effect of the processing technology on the wear behavior of Ti6Al4V alloy used in biomedical applications. The key importance of Ti6Al4V wear behavior on implants performance and the lack of comparative studies of this kind on literature are the motivation to this study.

2 Experimental

2.1 Materials and processing routes

HP and SLM Ti6Al4V specimens were produced using spherical Ti6Al4V powders (from SLM solutions supplier) having a mean particle size from 20 to 50 μm. The chemical composition of the Ti6Al4V alloy powder is given in Table 1.

Table 1 Chemical composition of Ti6Al4V alloy powder (mass fraction, %)

Al	V	C	Fe	O	N	H	Ti
6.4	3.8	0.01	0.23	0.12	0.02	0.0074	Bal.

2.1.1 Selective laser melting

Ti6Al4V specimens were fabricated using a commercial SLM equipment (SLM solutions, 125 HL) equipped with an Yb-Faser laser with a laser spot of 87 μm. The building chamber was firstly evacuated and filled with an inert gas (Ar/N_2). During the production, the platform base was maintained at 200 °C. The SLM processing parameters were laser power of 90 W, scan speed of 600 mm/s, scan spacing of 0.08 mm and layer thickness of 0.03 mm. It is important to highlight that the selected SLM conditions were defined based on a previous study where the most effective processing parameters were identified.

2.1.2 Hot pressing

Ti6Al4V specimens were produced by HP using a pressure-assisted sintering system [36] under a vacuum of 1×10^4 Pa. A pressure of 44 MPa was applied during 30 min at a temperature of 1175 °C.

2.1.3 Casting

Cast commercial Ti6Al4V alloy (from Bunting Titanium, UK) was used for obtaining cast Ti6Al4V specimens.

2.2 Microstructural and crystallographic analysis

The cast, HP and SLM Ti6Al4V specimens were prepared for microstructural observation by wet grounding with SiC abrasive papers down to 4000 grit, followed by polishing with diamond paste down to 1 μm. In order to reveal the microstructure, the specimens were etched with Kroll's reagent: 5% HNO_3, 10% HF and 85% distilled water.

The microstructures were assessed by using an optical microscope (Leica DM 2500M, Leica Microsystems, Germany) connected to a computer for image processing, using Leica Application Suite software (Leica Microsystems, Germany).

X-ray diffraction (XRD) measurement was performed using a Bruker AXS D8 Discover with Cu K_α radiation for each processing technology. A scanning angle (2θ) ranging from 30° to 90°, with a scan step of 0.05° and a counting time of 2 s was used.

The following relationship [10] was used to estimate the percentage of phases (α and β) on specimens obtained by each processing technology, using the intensities of reflection of X-ray diffraction data:

$$R_{(x)}=\left(\frac{I_{(x)}}{\sum I_{(x)}}\right)\times 100\% \quad (1)$$

where $R_{(x)}$ is the relative intensity of the phase; $I_{(x)}$ is the intensity of reflection corresponding to the x phase; and $\sum I_{(x)}$ is the sum of all the peaks intensities.

2.3 Hardness tests and wear tests

Vickers hardness tests were performed using a DuraScan equipment from EMCO-TEST Company, with a load of 3 N during 15 s. The obtained results are an average of six indentations per sample (for Ti6Al4V alloy produced by casting, HP and SLM).

A reciprocating ball-on-plate tribometer (Bruker−UMT−2) was used to evaluate the wear performance of Ti6Al4V/Al_2O_3 sliding pairs. SLM, HP and cast Ti6Al4V specimens were used as plates. The counter body consisted of an alumina ball (10 mm in diameter, from Ceratec Technical Ceramics – NL). The wear test parameters were normal load of 3 N, at a frequency of 1 Hz, and the total stroke length of 3 mm during 60 min. The wet wear tests were carried out with the specimens submerged in phosphate buffered saline (PBS) [10] fluid (Table 2) at 37 °C, mimicking the human body temperature.

Table 2 Composition of phosphate buffered saline solution used in this work (ρ/(g·L^{-1}))

NaCl	KCl	Na_2HPO_4	KH_2PO_4
8	0.2	1.44	0.24

Ti6Al4V specimens were prepared in order to obtain a mirror finish. Both ball and Ti6Al4V specimens were cleaned in an ultrasonic bath immersed in isopropyl alcohol for 15 min before and after the tests. After testing, the specific wear rate was estimated by measuring the lateral width of the wear scars and using empirical mathematical equations assuming that the wear tracks are formed by perfect ball geometry [37].

The wear tracks on Ti6Al4V plates (for each processing technology) were analyzed by means of SEM-EDS in order to assess the dominant wear mechanisms.

3 Results and discussion

3.1 Microstructural and crystallographic characterization

Figure 1 shows the microstructures of Ti6Al4V specimens processed by three technologies of casting, HP and SLM. Detail images of the microstructure of Ti6Al4V specimens produced by SLM are found in Fig. 2.

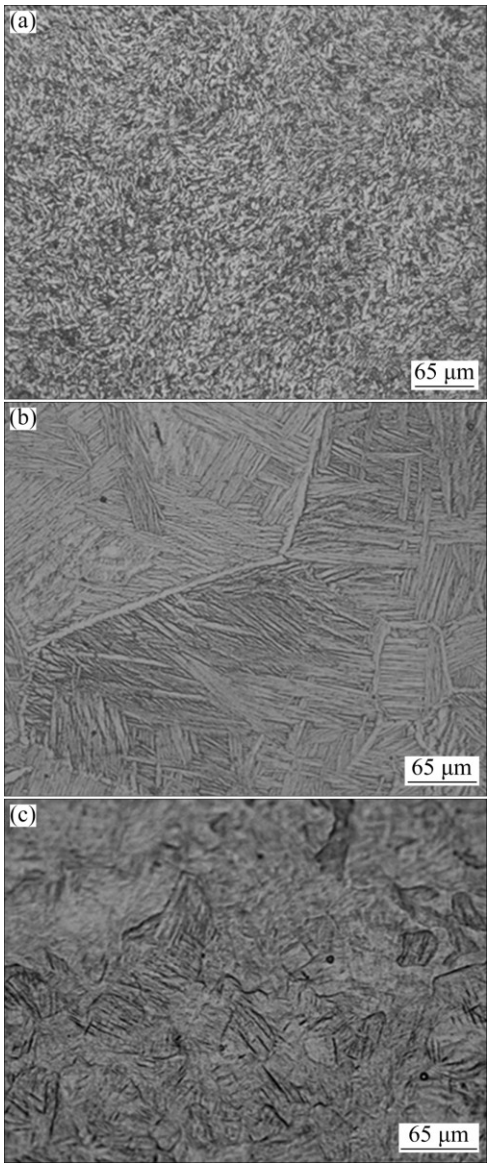

Fig. 1 Microstructures of Ti6Al4V specimens produced by three technologies: (a) Casting; (b) HP; (c) SLM

Figures 1 and 2 show noteworthy differences on the microstructures for Ti6Al4V specimens obtained by the three different processing technologies. In order to understand these differences, XRD analyses were performed (Fig. 3) for Ti6Al4V specimens fabricated by the three processes.

Figure 1(a) shows the microstructure of the Ti6Al4V sample obtained by casting route, exhibiting slightly elongated α grains (light) and intergranular β (gray) (as proven by the XRD pattern in Fig. 3(a)), having a measured grain size of (13±4) μm. Similar microstructures have been reported, on Ti6Al4V alloy fabricated by casting route [38]. This small grain size of material is due to the fact that after the continuous cast process the rods suffer a hot extrusion which leads to severe plastic deformation.

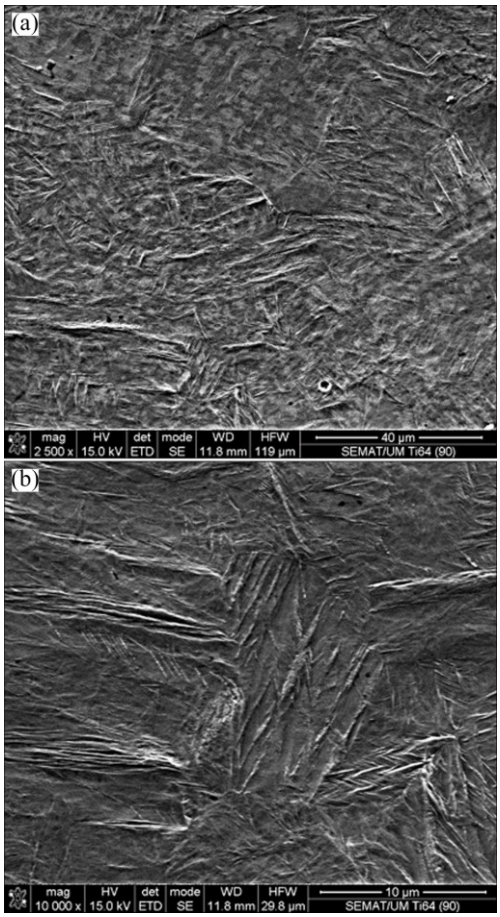

Fig. 2 Microstructures of Ti6Al4V specimens produced by SLM technology: (a) Lower magnification; (b) Higher magnification

Figure 1(b) shows the microstructure of the Ti6Al4V sample obtained by HP technology with a lamellar structure consisting of α+β phases (as seen in Fig. 3(b)) with a measured grain size of (287±4) μm. Similar microstructure was found in Refs. [17,18] on Ti6Al4V alloy fabricated by HP.

Figures 1(c) and 2 show the microstructures of the Ti6Al4V sample obtained by SLM, revealing a martensitic α' (α acicular) phase near the β grain boundaries, as reported by similar studies [1,19]. Although the presence of martensitic α' (α acicular phase) was confirmed in Fig. 2, XRD analysis was not able to detect α' phase, as α' and α phases present the same crystalline structure (hexagonal close packed) [10,19].

Equation (1) was used to obtain an estimative of the amount of each phase, for each type of sample (casting, HP and SLM). These results are shown in Fig. 4.

The results in Fig. 4 clearly show a higher amount of α phase for HP and SLM specimens, when compared with the cast ones. On the other hand, β phase was found more prevalent on specimens obtained by casting. Considering that the amount of retained β phase is dictated by the experienced cooling rate [34,35], the

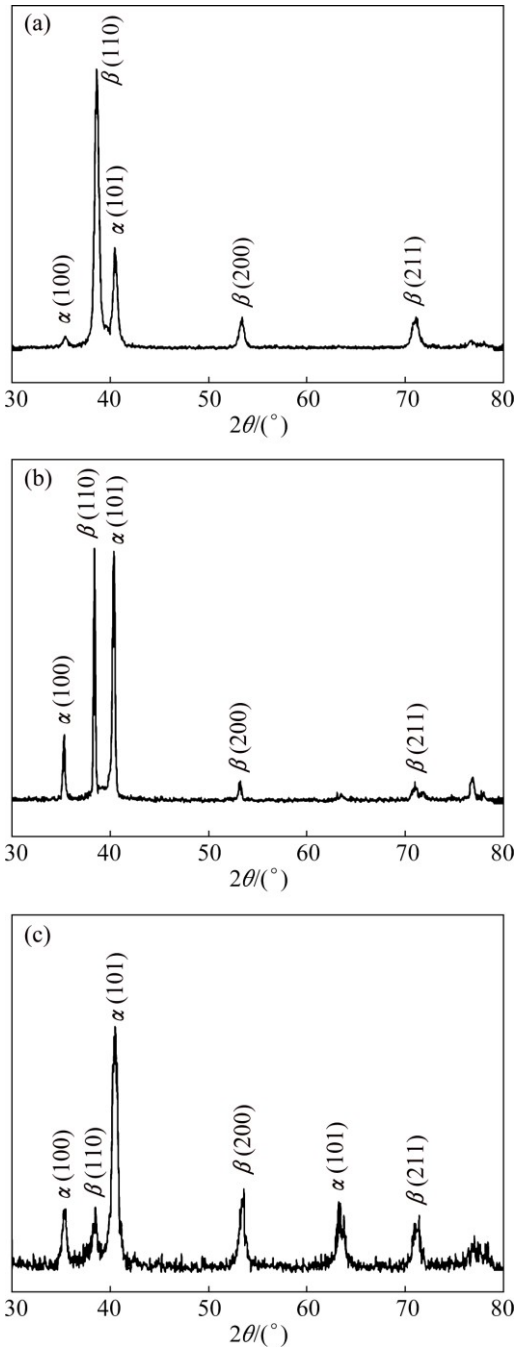

Fig. 3 XRD patterns of Ti6Al4V specimens obtained by three technologies: (a) Casting; (b) HP; (c) SLM

different cooling rates of each processing technology can explain the differences in the amount of α and β phases found among specimens produced by casting, HP and SLM.

As previously mentioned, Ti6Al4V specimens obtained by casting, were processed by a continuous casting process where liquid metal was solidified with a slow cooling rate (~0.5 K/s) [36,37], thus leading to a high concentration of β phase (Fig. 4). Ti6Al4V specimens obtained by HP, after being submitted to a sintering temperature higher than the $\beta_{transus}$ temperature,

experienced a cooling rate of 3 K/s. As reported by AHMED and RACK [39], a cooling rate between 1.5 and 20 K/s induced the transformation of β phase to α phase. This fact explains the obtained amount of α and β phases on HP specimens (Fig. 4).

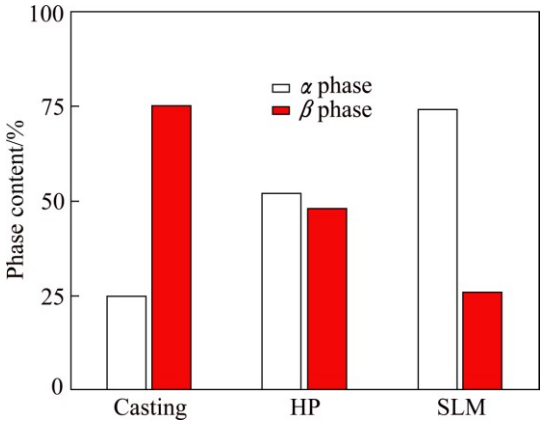

Fig. 4 Percentual contents of α and β phases for specimens obtained by casting, HP and SLM

By selective laser melting, energy is applied instantaneously, melting the powders and causing each produced layer to experience an extremely high cooling rate (10^3−10^6 K/s) [33,34]. During SLM, high temperature gradients are induced in the materials due to the high energy of the laser beam and the high cooling rates. These aspects can lead to thermal residual stresses, formed by the expansion and contraction of the previously solidified layers [21,30]. As a consequence, in SLM processing of Ti6Al4V there is enough time for solution-treated atom V in β phase to diffuse out of the cells, transforming into α phase instead. Although the martensite transformation is a diffusionless transformation which occurs at a speed close to the sound velocity, the BCC β phase is directly transformed into HCP α' phase [35], as proven in Fig. 2.

3.2 Hardness and specific wear rate

Figure 5 shows the hardness results for the specimens produced by different processing technologies. The average hardness obtained for the specimens fabricated by casting technology was HV (342±2). For HP specimens, the hardness value increased by 5% (HV (360±3)) and for SLM specimens the hardness value increased by 14% (HV (388±5)) when compared to casting.

The higher hardness values obtained for specimens produced by non-conventional technologies (HP and SLM) can be explained based on the constituents of microstructural phase. It has been reported that α' acicular phase is harder than α phase, which is harder than β phase [34,35]. Thus, higher hardness obtained for HP specimens is due to the higher amount of α phase and

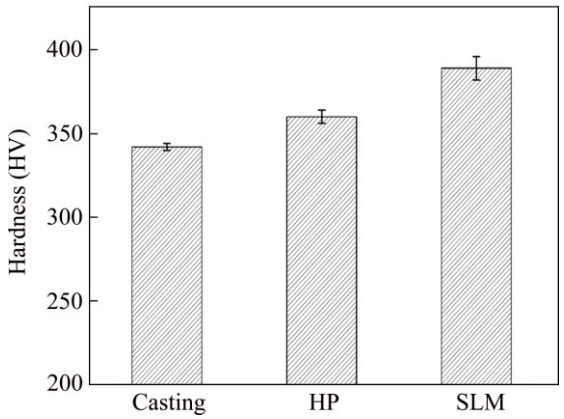

Fig. 5 Vickers hardness of Ti6Al4V specimens obtained by casting, HP and SLM

conversely the lower amount of β phase, when compared to specimens obtained by casting. On the other hand, the higher hardness of SLM specimens is also related with the presence of an acicular martensite microstructure, coherent to that described in Refs. [13,21]. Besides phase, other aspects such as grain size and density can influence the material hardness. In this sense, the density of Ti6Al4V specimens was measured by image analysis [27,31] and the following values were obtained: (99.82±0.15)% for casting, (99.67±0.26)% for HP and (99.74±0.24)% for SLM. By analyzing the results, it can be observed that an almost full densification on Ti6Al4V specimens produced by the three different technologies (casting, HP and SLM) was obtained. In this context, for these materials, there is a low influence of density on hardness, once they are all almost full densified. When concerning grain size, which was also measured by image analysis and taking cast and SLM specimens as example, similar grain sizes ((13±4) μm for casting and (14±5) μm for SLM) were obtained. By observing Fig. 5, noteworthy differences on the hardness values of Ti6Al4V produced by casting and SLM were obtained. According to the above mentioned facts, density and grain size alone cannot explain the differences found on hardness, with only the microstructural phase predominant in each material (casting, HP and SLM) justifying these hardness differences.

Figure 6 shows the specific wear rate measured for Ti6Al4V/Al_2O_3 sliding pairs, for Ti6Al4V plates obtained by casting, HP and SLM. It can be seen from Fig. 6 that processing route has a great effect on the wear performance of Ti6Al4V alloy, as the specific wear rates measured using Ti6Al4V alloy produced by non-conventional routes (HP and SLM) are lower than that of Ti6Al4V alloy produced by casting. When using Ti6Al4V plates produced by HP, the specific wear rate was 8% lower than that found for Ti6Al4V plates produced by casting. When using Ti6Al4V plates

produced by SLM, the specific wear rate was 21% lower than that found for Ti6Al4V plates produced by casting.

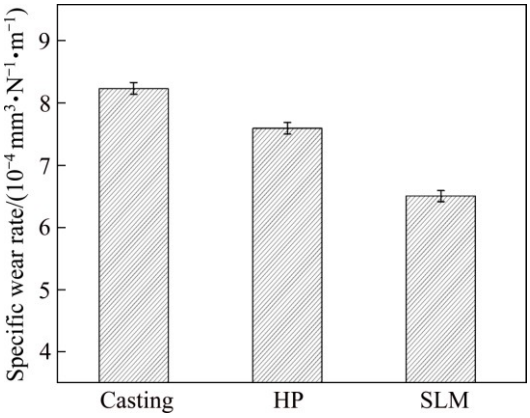

Fig. 6 Specific wear rate for Ti6Al4V plates obtained by casting, HP and SLM against Al_2O_3 ball

This higher wear resistance verified for specimens produced by non-conventional routes can be explained in terms of microstructural constituents and hardness. In fact, significantly lower wear loss of Ti6Al4V produced by SLM is related to the presence of acicular martensite that exhibits a significantly higher hardness [35] and consequently higher wear resistance. For Ti6Al4V produced by HP, the lower wear loss (compared with casting) is attributed to a higher amount of α phase on these specimens.

According to Archard's linear law [40], the wear volume loss is inversely proportional to the hardness values of the worn material. The hardness values of Ti6Al4V specimens produced by the three processing technologies studied in this work (Fig. 5) are coherent with the obtained wear rate results (Fig. 6), and totally in accordance with Archard's law.

3.3 Coefficient of friction

The evolution of the coefficient of friction (COF) during sliding of Ti6Al4V specimens produced by different processing technologies against Al_2O_3 balls, immersed in PBS solution, is shown in Fig. 7.

It can be observed that for all the different processing technologies, the COF attains the steady-state regime after a very short running-in period. Typical oscillations of the COF during the steady-state regime of the metal-on-metal sliding contacts are explained based on the third body effect [26].

When concerning the COF average values, no significant differences were found between Ti6Al4V produced by the different processing technologies. The average COF values obtained for Ti6Al4V/Al_2O_3 tribopair were: (0.387±0.01) for casting, (0.390±0.01) for HP and (0.398±0.01) for SLM. These values are aligned with other studies [11,41] where values close to 0.4 were obtained for Ti6Al4V (produced by casting, HP and SLM) sliding against alumina.

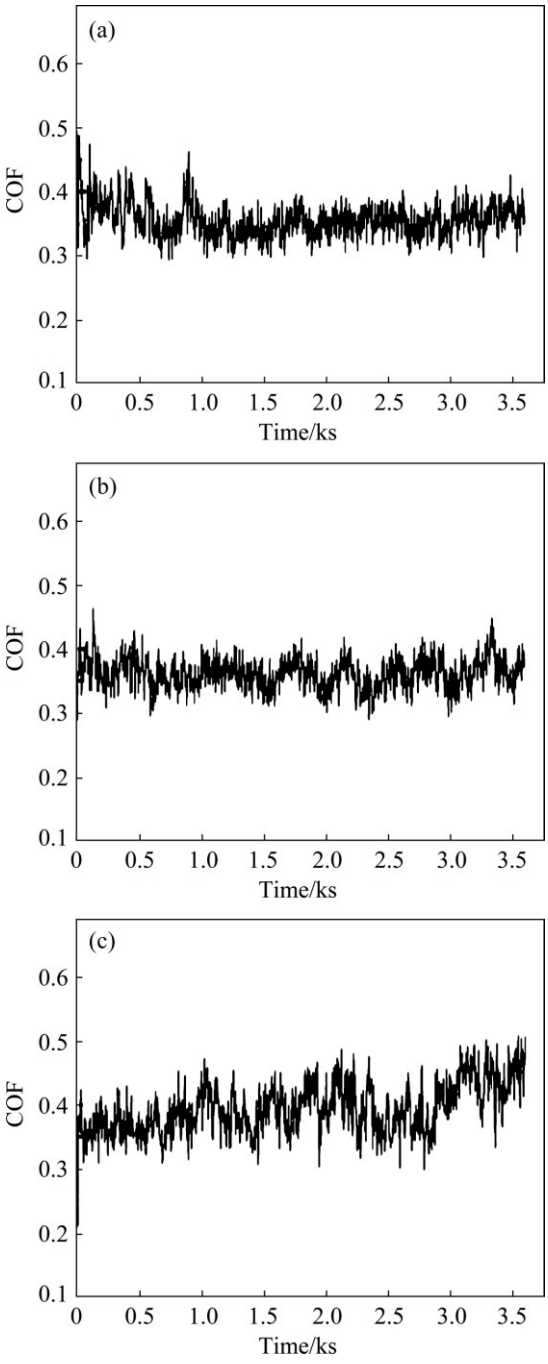

Fig. 7 Evolution of COF with sliding time for Ti6Al4V alloys obtained by different processing technologies: (a) Casting; (b) HP; (c) SLM

3.4 Wear tracks analysis

The wear tracks of Ti6Al4V plates obtained by casting, HP and SLM formed after the reciprocating sliding tests against Al_2O_3 balls, in the presence of PBS solution, were analyzed by means of SEM-EDS. The SEM images of these tracks are presented in Fig. 8, with the sliding direction indicated by arrows.

Figure 8 shows that sliding grooves are present on all the specimens, due to the occurrence of abrasive wear. It can be noted that the largest wear track was obtained on specimens produced by casting (Figs. 8(a_1)−(a_3). The wear track width and also the depth of the abrasion grooves are significantly minor on Ti6Al4V plates produced by SLM technology (Figs. 8(c_1)−(c_3)).

The wear tracks of Ti6Al4V specimen produced by casting (Figs. 8(a_1)−(a_3)) and HP (Figs. 8(b_1)−(b_3)) reveal a rougher appearance than that of specimens produced by SLM (Figs. 8(c_1)−(c_3)). The worn surface morphology of SLM specimens is relatively smooth, with slight grooves aligned parallel to the sliding direction (due to abrasion) (Figs. 8(c_1) and (c_2)). In this sense, Ti6Al4V specimens produced by casting and HP technologies reveal a greater surface degradation, coherent with the hardness results (lower hardness for casting, followed by HP) (Fig. 5) and specific wear rate (higher for casting, followed by HP) (Fig. 6).

Figure 9 shows SEM images of worn surfaces of Ti6Al4V plates using higher magnification. These images show darker areas that correspond to titanium oxides formed during sliding. The occurrence of oxidation is normal in titanium alloys, and it has been stated that it can lower the frictional force between the plate and the Al_2O_3 ball, lowering the coefficient of friction and acting like a diffusion barrier between the titanium plate and the Al_2O_3 ball [23,42]. On Ti6Al4V plates produced by SLM, less oxidized areas were found (as shown in Fig. 9(c)). EDS analysis confirmed that the darker areas in the wear tracks shown in Fig. 9 correspond to Ti-oxide, being a consequence of the sliding wear.

Regarding the wear mechanisms, the worn surfaces of all the Ti6Al4V specimens exhibited plastic deformation as a consequence of adhesive wear and also abrasive wear by the presence of grooves aligned along the sliding direction (Figs. 8 and 9).

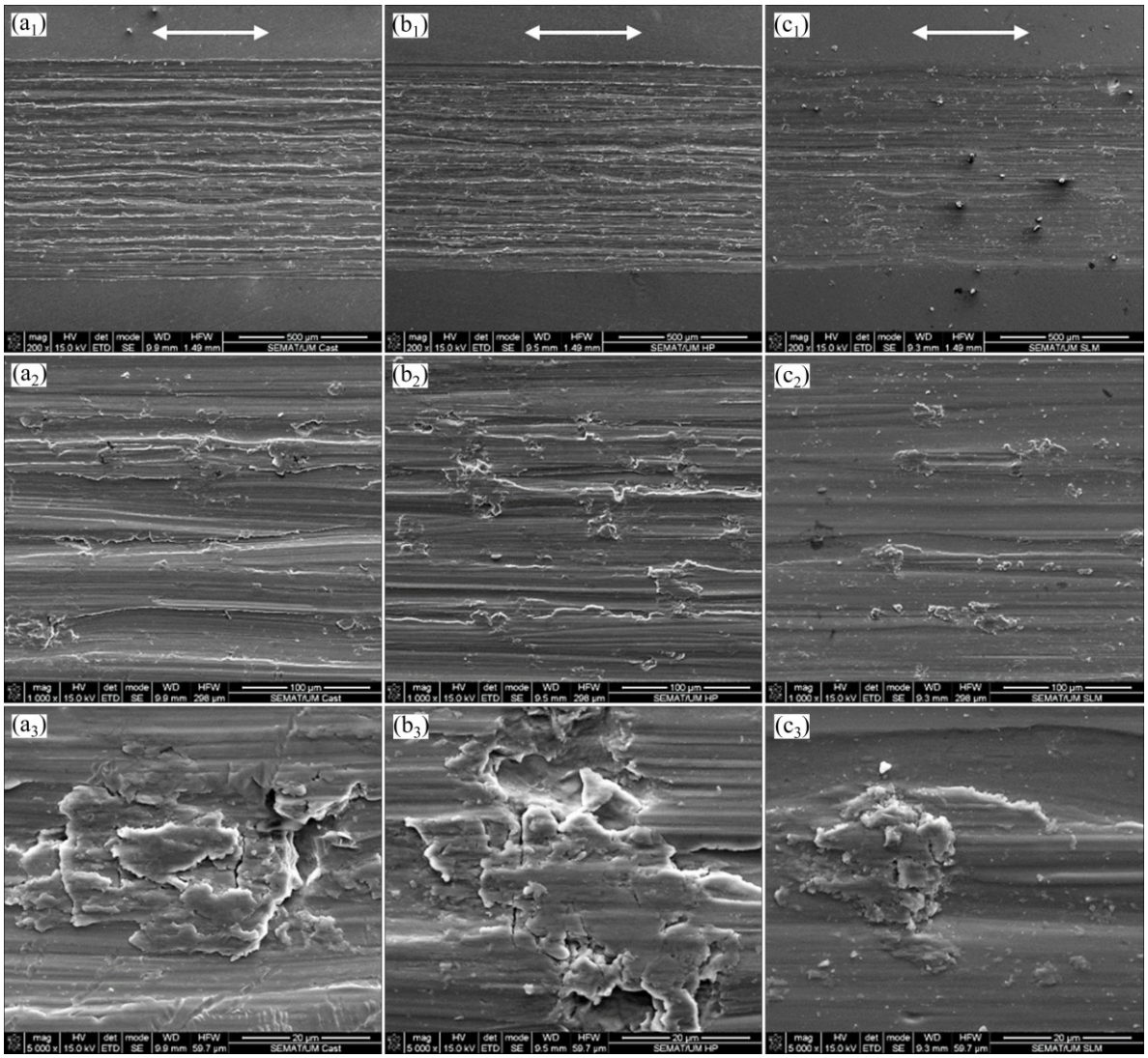

Fig. 8 SEM images of wear tracks formed after reciprocating sliding tests of Ti6Al4V alloy against Al_2O_3 balls in the presence of PBS solution: (a_1−a_3) Casting; (b_1−b_3) HP; (c_1−c_3) SLM

The relative extent of the grooves observed on the wear tracks depends on the hardness of the counter body. SEM images and EDS spectrum of the counter body (Al_2O_3 ball) surfaces after sliding against Ti6Al4V specimens produced by different processing technologies are shown in Fig. 10.

EDS analysis (Fig. 10) revealed that some materials transfer from the Ti6Al4V plates to the Al_2O_3 ball (lighter areas), observed for all the sliding pairs analyzed. EDS analysis revealed the presence of Al and O from the Al ball, as well as Ti and V coming from Ti6Al4V plates. The topographies of the Al balls are characterized by island-like plateaus (lighter areas), and it can be seen from Fig. 10 that more lighter areas dispersed in the case of the ball used for sliding against the Ti6Al4V plate produced by SLM, unlike the other balls (used against Ti6Al4V produced by casting and HP) where more transfer materials are localized. This aspect may explain the smoother grooves found on the Ti6Al4V plates produced by SLM.

In this sense, a direct correlation between microstructural constituents, hardness values and wear response of Ti6Al4V specimens produced by different technologies was obtained.

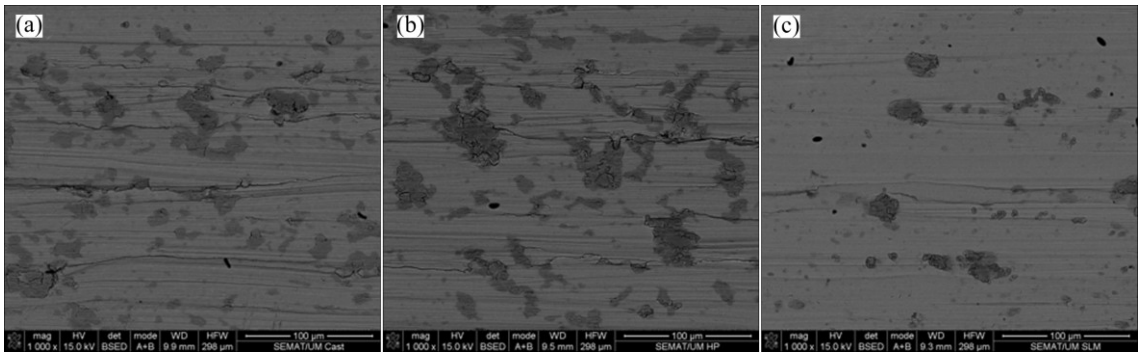

Fig. 9 SEM images of worn surfaces of Ti6Al4V specimens: (a) Casting; (b) HP; (c) SLM

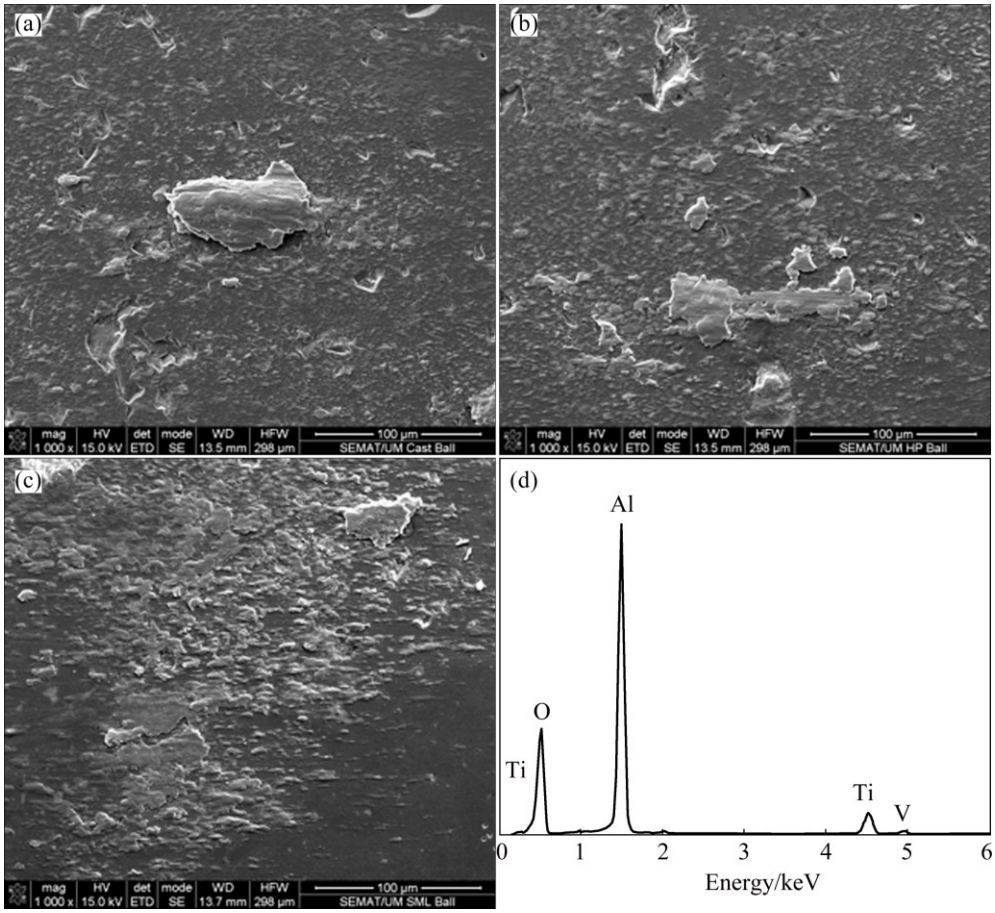

Fig. 10 SEM images (a−c) of counter body surface of Al_2O_3 ball surface (a−c for casting, HP and SLM, respectively) and typical EDS spectrum (d)

4 Conclusions

1) The distinctive cooling rate of each processing route was proven to affect microstructural phase constituents of Ti6Al4V specimen.

2) High cooling rate of selective laser melting leads to higher amount of α and α' harder phases on Ti6Al4V parts produced by this technology when compared to hot pressing and casting.

3) The presence of harder microstructural constituents on Ti6Al4V specimen produced by selective laser melting leads to a higher wear resistance.

4) The performance of Ti6Al4V parts produced by selective laser melting verifies the ability of this technology to produce customized Ti6Al4V implants with improved wear behavior.

Acknowledgements

This work is supported by FTC through the projects PTDC/EMS-TEC/5422/2014 and EXCL/EMS-TEC/0460/2012 and the grant SFRH/BPD/112111/2015. Additionally, this work is supported by FCT with the reference project UID/EEA/04436/2013, by FEDER funds through the COMPETE 2020−Programa Operacional Competitividade e Internacionalização (POCI) with the reference project POCI-01-0145-FEDER-006941.

References

[1] BANDYOPADHYAY A, ESPANA F, BALLA V K, BOSE S, OHGAMI Y, DAVIES N M. Influence of porosity on mechanical properties and in vivo response of Ti6Al4V implants [J]. Acta Biomater, 2012, 6: 1640−1648.

[2] REIG L, TOJAL C, BUSQUETS D J, AMIGÓ V. Microstructure and mechanical behavior of porous Ti6Al4V processed by spherical powder sintering [J]. Materials, 2013, 6: 4868−4878.

[3] BALOYI N M, POPOOLA A P I, PITYANA S L. Microstructure, hardness and corrosion properties of laser processed Ti6Al4V-based composites [J]. Transactions of Nonferrous Metals Society of China, 2015, 25: 2912−2923.

[4] CHEN Jun, ZHANG Qing, LI Quan-an, FI San-ling, WANG Jian-zhang. Corrosion and tribocorrosion behaviors of AISI 316 stainless steel and Ti6Al4V alloys in artificial seawater [J]. Transactions of Nonferrous Metals Society of China, 2014, 24: 1022−1031.

[5] YAN Y, NEVILLE A, DOWSON D. Biotribocorrosion — An appraisal of the time dependence of wear and corrosion interactions: I. The role of corrosion [J]. Journal of Physics D: Applied Physics, 2006, 39: 3200−3205.

[6] THOMANN U I, UGGOWITZER P J. Wear-corrosion behavior of biocompatible austenitic stainless steels [J]. Wear, 2000, 239: 48−58.

[7] PRUITT L A, CHAKRAVARTULA A M. Mechanics of biomaterials: Fundamental principles for implant design [M]. Cambridge: Cambridge University Press, 2012.

[8] GRANHI D, CENNI E, TRISOLINO G, GIONTI A, BALDINI N. Sensitivity to implant materials in patients undergoing total hip replacement [J]. J Biomed Mater Res, 2006, 77: 257−264.

[9] LIN Xiu-zhou, ZHU Min-hao, ZHENG Jian-feng, LUO Jun, MO Ji-liang. Fretting wear of micro-arc oxidation coating prepared on Ti6Al4V alloy [J]. Transactions of Nonferrous Metals Society of China, 2010, 20: 537−546.

[10] BALLA V K, SODERLIND J, BOSE S, BANDYOPADHYAY A. Microstructure, mechanical and wear properties of laser surface melted Ti6Al4V alloy [J]. J Mech Behav Biomed Mater, 2014, 32: 335−344.

[11] WENDLER B G, PAWLAK W. Low friction and wear resistant coating systems on Ti6Al4V alloy [J]. J Achiev Mater Manuf Eng, 2008: 26: 207−210.

[12] LONG M, RACK H J. Titanium alloys in total joint replacement—A materials science perspective [J]. Biomaterials, 1998, 19: 1621−1639.

[13] THIJS L, VERHAEGHE F, CRAEGHS T, HUMBEECK J V, KRUTH J P. A study of the microstructural evolution during selective laser melting of Ti−6Al−4V [J]. Acta Mater, 2010, 58: 3303−3312.

[14] RAFI H K, KARTHIK N V, GONG H, STARR T L, STUCKER B E. Microstructures and mechanical properties of Ti6Al4V parts fabricated by selective laser melting and electron beam melting [J]. J Mater Eng Perform, 2013, 22: 3872−3883.

[15] OLDANI C, DOMINGUEZ A. Titanium as a biomaterial for implants [M]. Houston: InTech, 2012.

[16] BOLZONI L, RUIZ-NAVAS E M, NEUBAUER E, GORDO E. Inductive hot-pressing of titanium and titanium alloy powders [J]. Mater Chem Phys, 2012, 131: 672−679.

[17] GRONOSTAJSKI Z, BANDOŁA P, SKUBISZEWSKI T. Influence of cold and hot pressing on densification behaviour of titanium alloy powder Ti6Al4V [J]. Arch Civ Mech Eng, 2009, 9: 47–57.

[18] BOZIC D, CVIJOVIC I, VILOTIJEVIC M, JOVANOVIC M. The influence of microstructural characteristics on the mechanical properties of Ti6Al4V alloy produced by the powder metallurgy technique [J]. J Serbian Chem Soc, 2006, 71: 985−992.

[19] ZHANG Sheng, WEI Qing-song, CHENG Ling-yu, LI Suo, SHI Yu-sheng. Effects of scan line spacing on pore characteristics and mechanical properties of porous Ti6Al4V implants fabricated by selective laser melting [J]. Mater Des, 2014, 63: 185−193.

[20] GU D D, HAGEDORN Y C, MEINERS W, MENG G B, SOUSA BATISTA R J, WISSENBACH K, POPRAWE R. Densification behavior, microstructure evolution, and wear performance of selective laser melting processed commercially pure titanium [J]. Acta Mater, 2012, 60: 3849−3860.

[21] SONG Bo, DONG Shu-juan, ZHANG Bai-cheng, LIAO Han-lin, CODDET C. Effects of processing parameters on microstructure and mechanical property of selective laser melted Ti6Al4V [J]. Mater Des, 2012, 35: 120−125.

[22] BORGIOLI F, GALVANETTO E, IOZZELLI F, PRADELLI G. Improvement of wear resistance of Ti−6Al−4V alloy by means of thermal oxidation [J]. Mater Lett, 2005, 59: 2159−2162.

[23] ZIVIC F, BABIC M, VENCL A. Continuous control as alternative route for wear monitoring by measuring penetration depth during linear reciprocating sliding of Ti6Al4V alloy [J]. J Alloys Compd, 2011, 509: 5748−5754.

[24] QIU Ming, ZHANG Yong-zhen, YANG Jian-heng, ZHU Jun. Microstructure and tribological characteristics of Ti−6Al−4V alloy against GCr15 under high speed and dry sliding [J]. Materials Science and Engineering A, 2006, 434: 71−75.

[25] ALAM M, HASEEB A S M A. Response of Ti−6Al−4V and Ti−24Al−11Nb alloys to dry sliding wear against hardened steel [J]. Tribology International, 2002, 35: 357−362.

[26] DONI Z, ALVES A C, TOPTAN F, GOMES J R, RAMALHO A, BUCIUMEANU M, PALAGHIAN L, SILVA F S. Dry sliding and tribocorrosion behaviour of hot pressed CoCrMo biomedical alloy as

compared with the cast CoCrMo and Ti6Al4V alloys [J]. Mater Des, 2013, 52: 47−57.
[27] MIRANDA G, FARIA S, BARTOLOMEU F, PINTO E, MADEIRA S, MATEUS A, CARREIRA P, ALVES N, SILVA F S, CARVALHO O. Predictive models for physical and mechanical properties of 316L stainless steel produced by selective laser melting [J]. Materials Science and Engineering A, 2016, 657: 43−56.
[28] REN Hai-shui, TIAN Xiang-jun, LIU Dong, LIU Jian, WANG Hua-ming. Microstructural evolution and mechanical properties of laser melting deposited Ti−6.5Al−3.5Mo−1.5Zr−0.3Si titanium alloy [J]. Transactions of Nonferrous Metals Society of China, 2015, 25: 1856−1864.
[29] XIAO Dong-ming, YANG Yong-qiang, SU Xu-bin, WANG Di, LUO Zi-yi. Topology optimization of microstructure and selective laser melting fabrication for metallic biomaterial scaffolds [J]. Transactions of Nonferrous Metals Society of China, 2012, 22: 2554−2561.
[30] SONG B, ZHAO X, LI S, HAN C, WEI Q, WEN S, LIU J, SHI Y. Differences in microstructure and properties between selective laser melting and traditional manufacturing for fabrication of metal parts: A review [J]. Front Mech Eng, 2015, 10: 111−125.
[31] BARTOLOMEU F, FARIA S, CARVALHO O, PINTO E, ALVES N, SILVA F S, MIRANDA G. Predictive models for physical and mechanical properties of Ti6Al4V produced by Selective Laser Melting [J]. Materials Science and Engineering A, 2016, 663: 181−192.
[32] OKAZAKI Y, GOTOH E. Comparison of metal release from various metallic biomaterials in vitro [J]. Biomaterials, 2005, 26: 11−21.
[33] SIMONELLI M, TSE Y Y, TUCK C. Effect of the build orientation on the mechanical properties and fracture modes of SLM Ti−6Al−4V [J]. Materials Science and Engineering A, 2014, 616: 1−11.
[34] ATTAR H, CALIN M, ZHANG L C, SCUDINO S, ECKERT J. Manufacture by selective laser melting and mechanical behavior of commercial pure titanium [J]. Materials Science and Engineering A, 2014, 593: 170−177.
[35] SUN Jian-feng, YANG Yong-qiang, WANG Di. Mechanical properties of a Ti6Al4V porous structure produced by selective laser melting [J]. Mater Des, 2012, 49: 545−552.
[36] MIRANDA G, CARVALHO O, SILVA F S, SORARES D. Effect of sintering stage in NiTi short-fibre-reinforced aluminium–silicon composites interface properties [J]. Journal of Composite Materials, 2013, 47: 1625−1631.
[37] SAMPAIO M, BUCIUMEANU M, HENRIQUES B, SILVA F S, SOUZA J C M, GOMES J R. Tribocorrosion behavior of veneering biomedical PEEK to Ti6Al4V structures [J]. J Mech Behav Biomed Mater, 2015, 54: 123−130.
[38] GEORGE F. ASM Handbook. Metallography and microstructure [M]. Volume 9. Ohio: ASM Int, 2001: 968−1015.
[39] AHMED T, RACK H J. Phase transformations during cooling in α+β titanium alloys [J]. Materials Science and Engineering A, 1998, 243: 206−211.
[40] HUTCHINGS I M. Tribology: Friction and wear of engineering materials [M]. Oxford: Butterworth-Heinemann, 1992.
[41] CHEN Jun, ZHANG Qing, LI Quan-an, FU San-ling, WANG Jian-zhang. Corrosion and tribocorrosion behaviors of AISI 316 stainless steel and Ti6Al4V alloys in artificial seawater [J]. Transactions of Nonferrous Metals Society of China, 2014, 24: 1022−1031.
[42] SOUZA J C M, HENRIQUES M, TEUGHELS W, PONTHIAUX P, CELIS J P, ROCHA L A. Wear and corrosion interactions on titanium in oral environment: Literature review [J]. J Bio Tribo Corros, 2015, 1: 13.

选择激光熔化、热压缩和传统铸造工艺加工的 Ti6Al4V 生物合金的磨损行为

F. BARTOLOMEU[1], M. BUCIUMEANU[2], E. PINTO[3], N. ALVES[3], F. S. SILVA[1], O. CARVALHO[1], G. MIRANDA[1]

1. Center for Microelectromechanical Systems (CMEMS), University of Minho, Azurém, 4800-058 Guimarães, Portugal;
2. Cross-Border Faculty of Humanities, Economics and Engineering, "Dunărea de Jos" University of Galaţi, Domnească 47, 800008 Galati, Romania;
3. Centre for Rapid and Sustainable Product Development Polytechnic Institute of Leiria, Rua General Norton de Matos, Apartado 4133, 2411-901 Leiria, Portugal

摘　要：本研究的主要目的是研究加工工艺对 Ti6Al4V 生物医学合金显微组织、硬度和摩擦学行为(摩擦和磨损行为)的影响。加工工艺包括传统铸造、热压缩和选择激光熔化。采用 X 射线衍射技术、维氏硬度测试和 Ti6Al4V/Al_2O_3 摩擦副的往复式球板磨损实验对 Ti6Al4V 生物医学合金的冶金、力学和摩擦学性能进行表征。结果表面，加工工艺路线对合金的显微组织、硬度和磨损行为的影响很大。采用选择激光熔化工艺获得的 Ti6Al4V 合金具有最高的硬度和最佳的耐磨性能，这是由于与采用热压缩和传统铸造工艺相比，选择激光熔化工艺具有显著不同的冷却速率，这使得合金具有明显不同的显微组织。本研究评估和证明选择激光熔化工艺在制备高耐磨 Ti6Al4V 生物植入体方面具有较大潜力。

关键词：生物医学合金；Ti6Al4V 合金；磨损行为；显微组织；选择激光熔化；热压缩；铸造

(Edited by Wei-ping CHEN)